PHYSICAL REVIEW D **88,** 074028 (2013)

QCD corrections to excited lepton (pair) production at the LHC

Swapan Majhi*

Department of Theoretical Physics, Indian Association for the Cultivation of Science, Kolkata 700032, India

(Received 14 February 2013; published 24 October 2013)

We consider the production of excited leptons ($\bar{l}^* l$ as well as $\bar{l}^* l^*$) at the LHC, followed by their two-body decay into standard model particles. We perform the next-to-leading-order QCD corrections to these processes. In spite of the nonrenormalizable nature of the interaction, such calculations are possible and meaningful. Not only are these corrections substantial and significant, the scale dependence of the next-to-leading-order cross section is greatly reduced as compared to that for the leading-order cross sections.

DOI: 10.1103/PhysRevD.88.074028 PACS numbers: 12.38.Bx, 12.38.−t, 12.60.−i

I. INTRODUCTION

The recent discovery of a Higgs-like scalar particle at the LHC may complete the most successful model in particle physics, namely, the standard model (SM). In spite of this huge success, there are other issues like the replication of the fermion families, dark matter, baryogenesis, etc., that are still not understood within the framework of the SM. To address these, one needs to consider physics beyond the SM. Some possible candidates are supersymmetry [1], grand unification [2,3] (with or without supersymmetry), family symmetries (gauged or otherwise), and quark-lepton compositeness [4]. The proliferation of fermion generations suggests the possibility of quarks and leptons being composite objects rather than elementary particles. In these theories [5,6], the fundamental constituents, *preons* [7], experience an additional strong and confining force. At energies far above a certain (compositeness) scale Λ, preons are almost free. Below this scale, the interaction of preons become very strong, forcing them to form bound states, namely, quarks and leptons. Understandably, in such models, higher (excited) states of quarks (q^*) and leptons (l^*) must also exist. At energies below Λ, the interaction of the l^* with the SM fermions can be parametrized in terms of an effective four-fermion Lagrangian given by [8]

$$\mathcal{L}_{CI} = \frac{2\pi}{\Lambda^2} \sum_{i,j=L,R} [\eta_{ij}(\bar{q}_i \gamma_\mu q_j)(\bar{l}_i^* \gamma^\mu l_j) + \eta'_{ij}(\bar{q}_i \gamma_\mu q_j)(\bar{l}_i^* \gamma^\mu l_j^*) + \text{H.c.}], \quad (1)$$

where l represents the SM lepton. In the above, we have not explicitly accounted for the full $SU(2)_L \times U(1)_Y$ invariance of the couplings, but this is to be understood, for the scale of compositeness has to be larger than the electroweak scale. This implies that not only would we produce, say, $\bar{e}^* e^*$ and $\bar{e}^* e$, but also $\bar{e}^* \nu_e^*$, $\bar{e}^* \nu_e$, and $\bar{\nu}_e^* e$.

The excited fermions can also be transformed into ordinary SM fermions through the gauge bosons. The effective gauge-mediated Lagrangian [8,9] between a SM fermion F and its excited counterpart F^* is given by

$$\mathcal{L}_{\text{GM}} = \frac{1}{2\Lambda} \bar{F}_R^* \sigma^{\mu\nu} \left[g_s f_s \frac{\lambda^a}{2} G^a_{\mu\nu} + g f'' \frac{\tau}{2} . W_{\mu\nu} + g' f' \frac{Y}{2} B_{\mu\nu} \right] F_L + \text{H.c.}, \quad (2)$$

where $G^a_{\mu\nu}$, $W_{\mu\nu}$, and $B_{\mu\nu}$ are the field strength tensor of the $SU(3)$, the $SU(2)$, and the $U(1)$ gauge fields, respectively. The parameters f_s, f'', and f' are usually of the order of unity.

It is evident that these operators may lead to significant phenomenological effects in collider experiments such as e^+e^- [10], eP [11], or hadronic [12–14]. It is quite obvious that the effects would be more pronounced at higher energies, given the higher-dimensional nature of $\mathcal{L}_{CI}$ and $\mathcal{L}_{\text{GM}}$. The best low-energy bounds on such a composite operator would arise from the precise measurement of leptonic branching ratios (BR) of the τ [15]. Similarly, loops with these excited states can significantly modify rare processes, and a comparison with the experimental data can impose bounds on their masses and couplings. These bounds, though, are quite weak [16]. The best direct constraints on such excited states come from the Delphi [10] and CDF [12] experiments. For the contact interaction scale $\Lambda = 1$ TeV, CDF has excluded the excited electron mass below 756 GeV at the 95% C.L. More recently, the measurement of the $\bar{l}l\gamma$ cross section [13,14] at high invariant masses set the most stringent limits on contact interactions of the type given in Eq. (2). For $\Lambda = M_*$, CMS has excluded excited electrons below 1070 GeV and excited muons below 1090 GeV at the 95% C.L. For higher values of contact interaction scale (viz. $\Lambda = 2$ TeV), the excited lepton mass has been excluded below 760 GeV for electrons and 780 GeV for muons.

It is a well-known fact that QCD corrections can alter, quite significantly, generic cross sections at hadron colliders. Even for a simple process like Drell-Yan [17], the leading-order (LO) approximation is a serious underestimation, forcing us to incorporate at least the

*tpskm@iacs.res.in

next-to-leading-order (NLO) or, better, next-to-leading log [18,19] results in Monte Carlo codes [18] or event generators such as JETRAD [20] and HERWIG [21]. It is expected that such corrections would be important in the context of other processes as well. Recently, the above-mentioned contact interactions have received much attention from both the CMS [13] and ATLAS [14] Collaborations. They have searched for heavy excited leptons via the $\bar{l}l\gamma$ channel and put a bound on its mass. However, there exists no higher-order calculations for this process, and, consequently, all collider searches of contact interaction either have been based on leading-order calculations or have assumed that the higher-order corrections are exactly the same as for the SM process. In this article, we aim to rectify this unsatisfactory state of affairs. While it may seem that the NLO corrections to the processes driven by such nonrenormalizable interactions are ill defined, it is not quite true [22,23]. In particular, if the interaction can be factorized into a current-current form, with colored fields appearing in only one current, then the NLO QCD corrections affect only this current and can be computed without any difficulties. For example, Ref. [22] dealt with contact interactions involving the SM fermions alone.

The rest of the article is organized as follows. In Sec. II, we start by outlining the general methodology and follow it up with the explicit calculation of the NLO corrections to the differential distribution in the dilepton ($\bar{l}^* l$, $\bar{l}^* l^*$) invariant mass. In Sec. III, we present our numerical results. Finally, we summarize in Sec. IV.

II. NLO CORRECTIONS

We consider excited leptons production in the context of contact interaction as exemplified by Eqs. (1) and (2) at the LHC. The processes are

$$P(p_1)+P(p_2) \;\to\; \overset{(-)}{l^*}(l_1)+\overset{(\,)}{\bar{l}}(l_2)+X(p_X) \qquad \text{(3)}$$
$$\qquad\qquad\qquad\quad \hookrightarrow \overset{(-)}{l}(l_3)+V(p_4)\,,$$

$$P(p_1)+P(p_2) \;\to\; \bar{l}^*(l_1)\;\; l^*(l_2)+X(p_X) \qquad \text{(4)}$$
$$\qquad\qquad\qquad\quad \hookrightarrow l(l_4)+V(p_5)$$
$$\qquad\qquad\qquad\quad \hookrightarrow \bar{l}(l_3)+V'(p_4)\,,$$

where p_i $(i=1,2)$ denote the momenta of the incoming hadrons and l_i those for the outgoing leptons. Similarly, the outgoing vector bosons V, $V'(=\gamma, Z, W)$ have momenta $p_{4,5}$, whereas the inclusive hadronic final state carries p_X. In the above-mentioned processes, we have considered only two-body leptonic decays of the excited leptons.[1] The hadronic cross section is defined in terms of the partonic cross section convoluted with the appropriate parton distribution functions $f_a^P(x)$ and is given by

$$2S\frac{d\sigma^{P_1P_2}}{dQ^2} = \sum_{ab=q,\bar{q},g}\int_0^1 dx_1\int_0^1 dx_2 f_a^{P_1}(x_1)f_b^{P_2}(x_2) \times\int_0^1 dz\, 2\hat{s}\frac{d\sigma^{ab}}{dQ^2}\,\delta(\tau - zx_1x_2), \qquad (5)$$

where x_i is the fraction of the initial state proton's momentum carried by the ith parton. For the sake of completeness,

$$S\equiv(p_1+p_2)^2, \qquad \hat{s}\equiv(k_1+k_2)^2,$$
$$Q^2\equiv(l_1+l_2)^2, \qquad \tau\equiv\frac{Q^2}{S}, \qquad (6)$$
$$z\equiv\frac{Q^2}{\hat{s}}, \qquad \tau\equiv zx_1x_2.$$

At first glance, the nonrenormalizable nature of the effective Lagrangian threatens to come in the way of reliably calculating loops. However, the fact that it can resolved into a product of a hadronic current with a nonhadronic one allows us to factorize the QCD corrections. These affect only the hadronic current, with the latter being a dimension-three operator. With the leptonic tensor being a mute spectator, the offending higher-dimensional nature of the effective Lagrangian never comes into play.

Of particular interest is the leptonic tensor with two massive final state particles, namely,

$$L^{jj'\to ll'} = \int\prod_i^2\left(\frac{d^n l_i}{(2\pi)^n}2\pi\delta^+(l_i^2-m_i^2)\right) \times(2\pi)^n\delta^{(n)}(q-l_1-l_2)|\mathcal{M}^{jj'\to l^*l'}|^2, \qquad (7)$$

which leads to

$$L_{jj'\to l^*l'} = \left(-g_{\mu\nu}+\frac{q_\mu q_\nu}{Q^2}\right)L_{l^*l'}(Q^2) \qquad (l'=l,l^*), \qquad (8)$$

with

$$L_{l^*l}(Q^2) = \frac{1}{12}\left(Q^2-\frac{m_1^2+m_2^2}{2}-\frac{(m_1^2-m_2^2)^2}{2Q^2}\right). \qquad (9)$$

To calculate the Q^2 distribution of the excited lepton pair ($\bar{l}^* l^*$ or $\bar{l}^* l$), one needs to calculate the hadronic tensor as well. For this part of our calculation, we have followed the procedure of Ref. [22]. The physical hadronic cross section can be obtained by convoluting the finite coefficient functions with appropriate parton distribution functions, and hence the inclusive differential cross section is given by

[1] Also possible are three-body decays through the four-Fermi interactions with their own QCD corrections. We postpone a discussion of this issue to a later study [24].

$$2S\frac{d\sigma^{P_1P_2}}{dQ^2}(\tau, Q^2) = \sum_q \int_0^1 dx_1 \int_0^1 dx_2 \times \int_0^1 dz\,\delta(\tau - zx_1x_2)\mathcal{F}^{VA}\mathcal{G}_{VA},$$
$$\mathcal{G}_{VA} \equiv H_{q\bar{q}}(x_1, x_2, \mu_F^2)\{\Delta_{q\bar{q}}^{(0),VA}(z, Q^2, \mu_F^2) + a_s\Delta_{q\bar{q}}^{(1),VA}(z, Q^2, \mu_F^2)\} + \{H_{qg}(x_1, x_2, \mu_F^2) + H_{gq}(x_1, x_2, \mu_F^2)\}a_s\Delta_{qg}^{(1),VA}(z, \mu_F^2), \quad (10)$$

where the renormalized parton flux $H_{ab}(x_1, x_2, \mu_F^2)$ and the finite coefficient functions $\Delta_{ab}^{(i)}$ are given in Refs. [22,23,25]. The effective coupling $\mathcal{F}^{VA}$ contains information of all the couplings, propagators, and the massive final state particles and is given by

$$\mathcal{F}^{VA} = \frac{|\eta|^2\beta}{12}\frac{Q^2}{\Lambda^4}\left\{1 - \frac{(m_1^2 + m_2^2)}{2Q^2} - \frac{(m_1^2 - m_2^2)^2}{2Q^4}\right\}, \quad (11)$$

$$\beta = \left(1 + \frac{m_1^4}{Q^4} + \frac{m_2^4}{Q^4} - 2\frac{m_1^2}{Q^2} - 2\frac{m_2^2}{Q^2} - 2\frac{m_1^2}{Q^2}\frac{m_2^2}{Q^2}\right)^{\frac{1}{2}}. \quad (12)$$

III. RESULTS AND DISCUSSION

In the previous section, we have calculated the differential distribution with respect to the invariant mass of the leptonic pair (either $\bar{l}^*l$ or $\bar{l}^*l^*$). The total cross section is trivially obtained by integrating over Q^2, namely,

$$\sigma^{P_1P_2}(M_*^2, S, \Lambda) = \int \frac{d\sigma^{P_1P_2}(\tau, Q^2)}{dQ^2}dQ^2. \quad (13)$$

We present our numerical results for three different LHC energies, namely, $\sqrt{S} = 7$, 8, 14 TeV. We start by making the simplest choice for the renormalization and the factorization scale, viz. $\mu_R^2 = \mu_F^2 = Q^2$, and postpone a discussion on the dependence on $\mu_{R,F}$ until later. Since the QCD correction does not depend on the contact interaction scale Λ, for definiteness we use a particular value, namely, $\Lambda = 6$ TeV, unless it is quoted to be otherwise. Similarly, all the coupling constants η_{ij} and the f's are also held to unity. While the main findings of this paper are essentially independent of these specific values for the parameters, the latter have been chosen so as to facilitate a quick and easy comparison with the experimental analyses existing in the literature. For the same reason, we use the Cteq6Pdf [26] parton distribution functions (PDFs), unless specifically mentioned otherwise. Thus, the LO hadronic cross section is obtained by convoluting the LO parton distribution function (namely, Cteq6l1) with the LO partonic cross section, and for the NLO hadronic cross section, we convolute the NLO parton distribution (namely, Cteq6m) with the NLO partonic cross section. The corresponding QCD scale is $\Lambda_{\rm QCD} = 0.226(0.165)$ GeV for NLO (LO) for $n_f = 5$.

To start with, we discuss the NLO corrections to $\bar{l}^*l$ (this, by definition, includes $\bar{l}l^*$ as well) and $\bar{l}^*l^*$ production in general, specializing later to a particular final state, namely, $\bar{l}l\gamma$, which has been analyzed by both the CMS [13] and ATLAS [14] Collaborations. In the context of the excited lepton, this final state is primarily attained through the production and subsequent decay of an l^*. As the decay is free of any QCD correction, the NLO QCD correction to the full process, namely, $\bar{l}l\gamma$ production, is essentially the same as that for on-shell $\bar{l}^*$ production.

In Fig. 1, we have plotted the total cross section for both single and pair production of excited leptons, as a function of its mass M_*. In calculating the same, we have assumed that the four-Fermi operators are flavor democratic, i.e., the couplings η_{ij} (η'_{ij}) are independent of the quark flavor. In other words, the cross sections in Fig. 1 contain the contributions of all of the light quarks (u, d, s), with those of the heavier quarks being essentially negligible. The contribution of the individual light quark is depicted in Fig. 2.

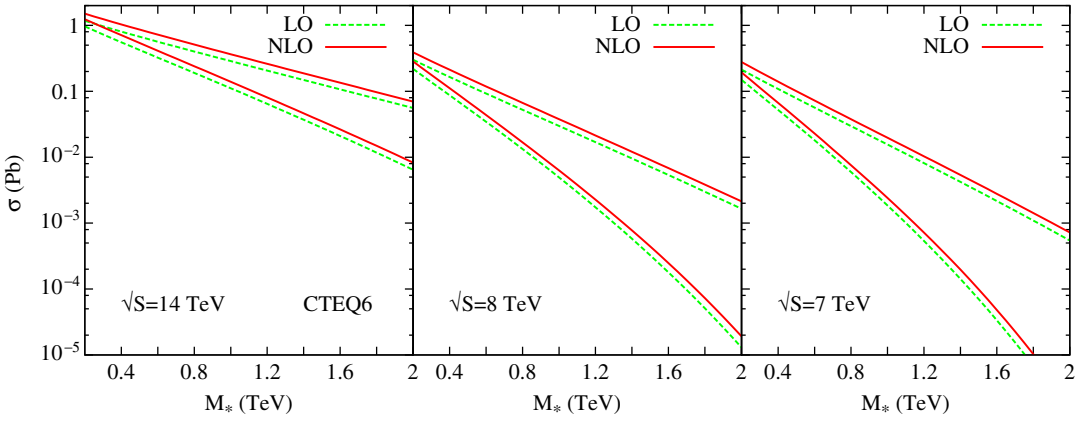

FIG. 1 (color online). Variation of the total cross section for $\bar{l}^*l^*$ and $\bar{l}^*l$ production with respect to excited lepton mass (M_*) at the LHC. For each set, the solid (dashed) lines refer to NLO (LO) cross sections. The upper (lower) set represents $\bar{l}^*l$ ($\bar{l}^*l^*$) for $\Lambda = 6$ TeV.

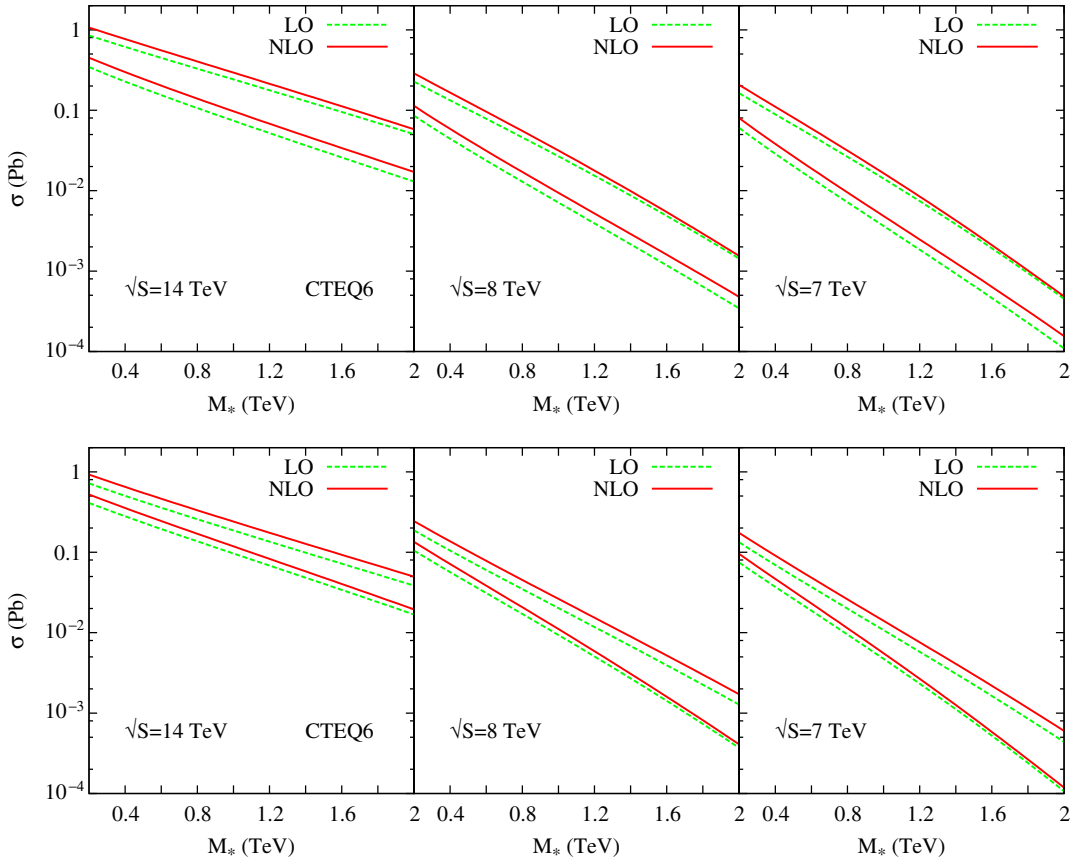

FIG. 2 (color online). Variation of the individual total cross section for $\bar{l}^* l$ production with respect to the excited lepton mass (M_*) at the LHC. For each set, the solid (dashed) lines refer to NLO (LO) cross sections. In the upper panel, the upper (lower) set represents the $u\bar{u}(d\bar{d})$ initiated process, and in the lower panel, the upper (lower) set represents the $u\bar{d}(d\bar{u})$ initiated process at the Born level for $\Lambda = 6$ TeV.

The decrease of the cross sections with M_* is not only due to the fall of the partonic cross sections, but also due to the fall in effective flux of the $q\bar{q}$ pair (relevant for both the LO and the NLO calculations) as well as the qg pair (relevant for NLO alone) with increasing parton momentum fractions. Understandably, the fall of the total cross section is faster for lower center of mass (c.o.m.) energies $\sqrt{S}(\equiv 7, 8$ TeV) than the higher c.o.m. energy $\sqrt{S}(\equiv 14$ TeV). As expected, the $\bar{l}^* l^*$ production cross section both is lower than and falls faster compared to the $\bar{l}^* l$ production cross section. All the cross sections (Figs. 1 and 2) have similar qualitative features (though the actual numbers are quite different), a reflection of the flavor independence of the underlying dynamics.

To quantify the enhancement of the NLO cross section, we define a variable called the K factor as given by

$$K_i = \frac{\sigma_i^{\mathrm{NLO}}}{\sigma_i^{\mathrm{LO}}}, \qquad i = \text{total}, u\bar{u}, d\bar{d}, u\bar{d}, d\bar{u}, \tag{14}$$

where the LO (NLO) cross sections are computed by convoluting the corresponding parton-level cross sections with the LO (NLO) parton distribution functions.

In Figs. 3 and 4, we have shown the variation of the K factor with respect to M_*. The variation of the total K factor is about 25%–30% for moderate values of M_* (≤ 1 TeV) at low c.o.m. energies ($\sqrt{S} = 7, 8$ TeV) in Fig. 3. At a larger mass region ($M_* > 1$ TeV), the K factor rises very fast (25%–60%). At high c.o.m. energy ($\sqrt{S} =$ 14 TeV), the variation of the K factor is about 25%–30% for even larger masses ($M_* \leq 2$ TeV). Figure 4 shows the variation of the K factor for individual flavors only for the $\bar{l}^* l$ production process. In Figs. 3 and 4, the rate of change of the K factor is much slower at higher c.o.m. energy (say, $\sqrt{S} = 14$ TeV) than the lower c.o.m. energies. This is a consequence of the fact that at lower c.o.m. energies we are forced to higher momentum fractions and, hence, are integrating over smaller phase space regions. As the Bjorken x increases towards unity, the parton distribution function falls very steeply This is the reason why, at lower c.o.m. energies, the K factor increases very fast as mass M_* increases towards the center of mass energy. One can also see from Fig. 4 that the numerical difference between the individual flavor K factors is due to their respective flux difference. Since the d-quark parton density falls faster than the u-quark parton density with scale, the K factor

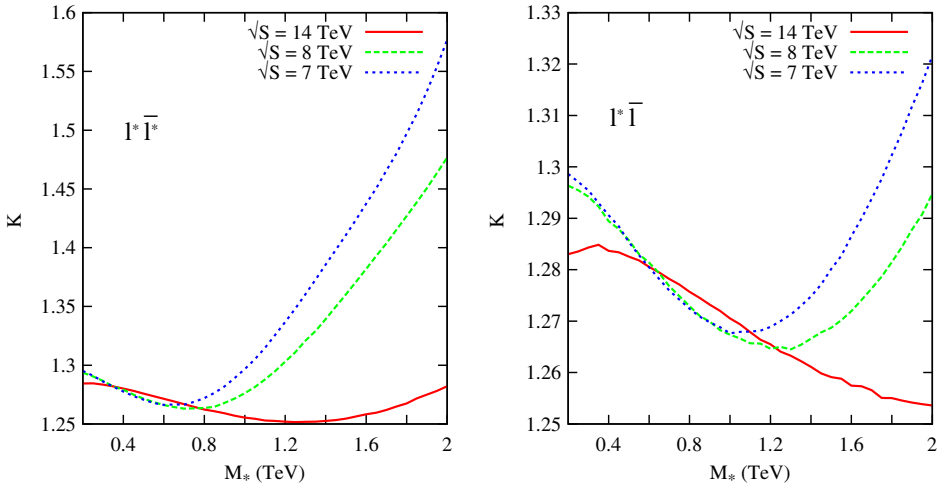

FIG. 3 (color online). Variation of the K factor with respect to the excited lepton mass (M_*) for $\Lambda = 6$ TeV at the LHC.

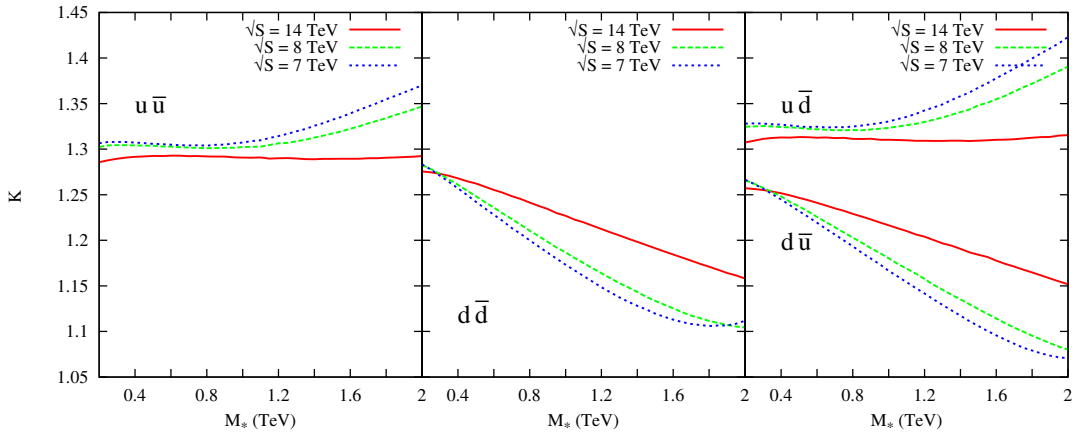

FIG. 4 (color online). Variation of the individual K factor with respect to the excited lepton mass (M_*) for $\Lambda = 6$ TeV at the LHC.

falls more steeply for $d\bar{d}$ initiated processes than $u\bar{u}$ initiated processes. This also explains the variation of the K factor for $d\bar{u}$ and $u\bar{d}$ processes with the earlier processes, the flux dominated by the valence d quark and later the flux dominated by the valence u quark.

A. $\bar{l}l\gamma$ production

The excited heavy lepton will decay into a light SM lepton and an electroweak gauge boson $V(\equiv \gamma, Z, W)$ according to the Lagrangian of Eq. (2). Therefore the total NLO cross section of the lepton pair ($\bar{l}l$) and a gauge boson V can be calculated by multiplying the branching ratio to Eq. (13) as given below:

$$\sigma^{P_1P_2}(M_*^2, S, \Lambda) = \mathrm{BR}(l^* \to lV) \int \frac{d\sigma^{P_1P_2}(\tau, Q^2)}{dQ^2} dQ^2. \tag{15}$$

The partial decay width of the excited lepton for various electroweak gauge bosons is given by

$$\Gamma(l^* \to lV) = \frac{1}{8}\alpha f_V^2 \frac{M_*^2}{\Lambda^2}\left(1 - \frac{m_V^2}{M_*^2}\right)\left(2 + \frac{m_V^2}{M_*^2}\right), \tag{16}$$

with

$$f_\gamma = f'' T_3 + f' \frac{Y}{2}, \tag{17}$$

$$f_Z = f'' T_3 \cot\theta_W - f' \frac{Y}{2} \tan\theta_W, \tag{18}$$

TABLE I. Decay widths of excited lepton and branching ratio $\mathrm{BR} = \Gamma(l^* \to l\gamma)/\Gamma(l^* \to \mathrm{all})$ for $\eta_{ij} = f'' = f' = 1$ and $\Lambda = 2$ TeV. Γ_{tot} represents the total decay width.

M_* (GeV)	$\Gamma_{\mathrm{tot}}/M_*$	$\Gamma_G/\Gamma_{\mathrm{tot}}$	$\Gamma_{CT}/\Gamma_{\mathrm{tot}}$	$\mathrm{BR}(l^* \to l\gamma)$
400	3.85×10^{-4}	0.6557	0.3443	0.1894
600	1.25×10^{-2}	0.4649	0.5351	0.1308
800	3.17×10^{-2}	0.3303	0.6697	0.0911
1000	6.82×10^{-2}	0.2407	0.7593	0.0668
2000	8.94×10^{-2}	0.0738	0.9262	0.0204

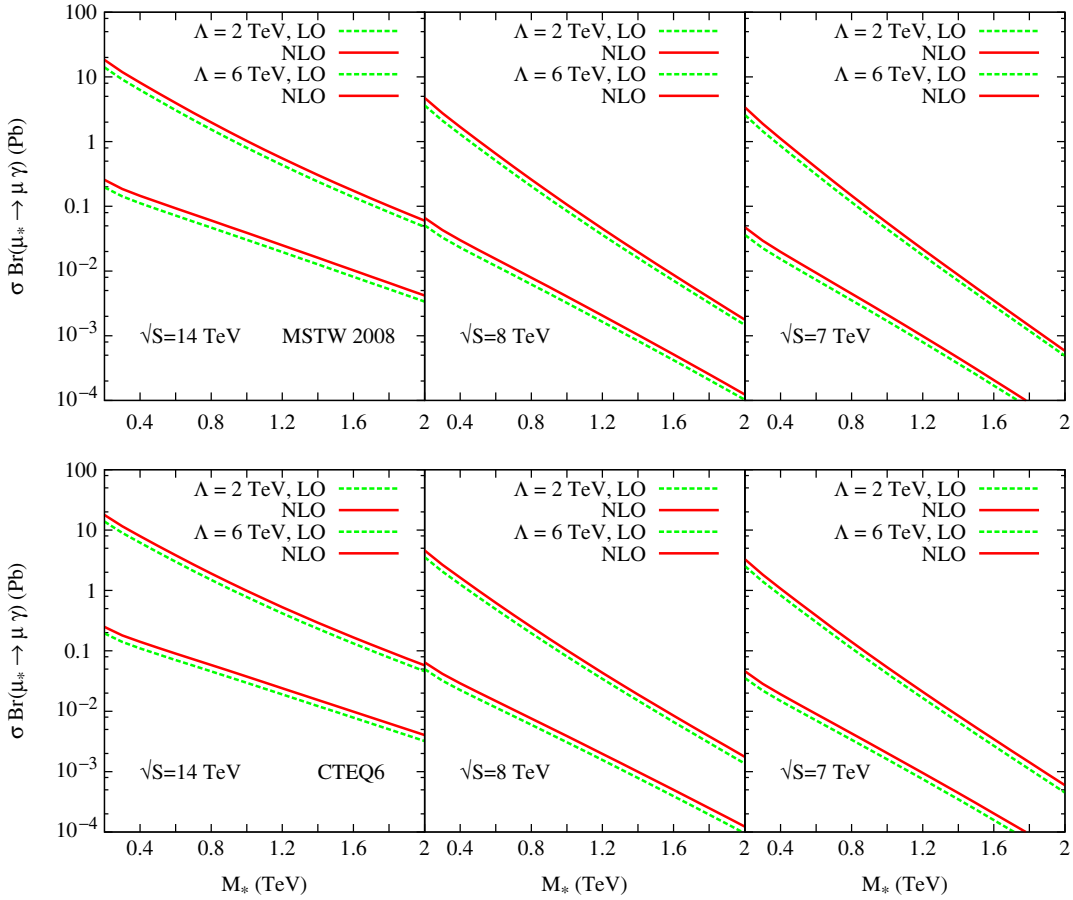

FIG. 5 (color online). Total cross section for $l\bar{l}\gamma$ production at the LHC. For each set, the solid (dashed) lines refer to NLO (LO) cross sections. The upper (lower) set is for $\Lambda = 2$ (6) TeV.

$$f_W = \frac{f''}{\sqrt{2}} \csc\theta_W, \tag{19}$$

where T_3 denotes the third component of the weak isospin and Y represents the weak hypercharge of the excited lepton. θ_W is Weinberg's angle. The compositeness parameters f'' and f' are taken to be unity throughout our analysis. The variation of these parameters has been considered elsewhere (for example, in Refs. [27,28]). The decay of the excited lepton mediated by electroweak interaction is mostly dominated by the W boson and a SM lepton. For a sufficiently large excited lepton mass (at least larger than m_W and m_Z), the branching ratios are insensitive to M_*. However, this is not quite true when one

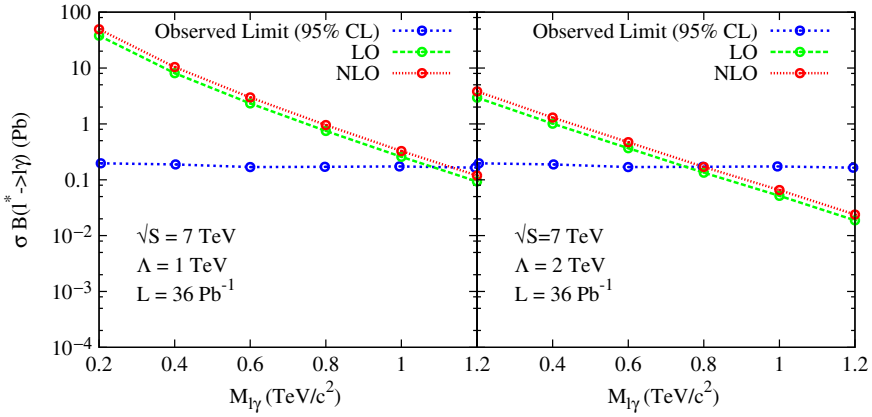

FIG. 6 (color online). Variation of the total cross section times branching fraction with excited lepton mass [red (short-dashed), green (dashed)] and blue (dotted) line is the observed limit (95% C.L.) taken from CMS [13].

TABLE II. Mass limit for the excited lepton. The number within the first bracket represents the CMS result.

		Excited lepton mass (GeV)	
Λ (TeV)	σ (Pb)	LO	NLO
1	0.173	1077 (1070)	1137
2	0.174	748 (760)	804

considered the three-body decay through contact interactions. In this case, the decay width of contact interaction (Γ_{CT}) is dominated over the width of electroweak interaction (Γ_G) as the mass of excited lepton increases, which is shown in Table I.

In Fig. 5, we have plotted the total cross section versus the invariant mass of a SM lepton and a photon $M_*(\equiv M_{l\gamma})$ for two different PDFs, namely, CTEQ6 [26] and MSTW

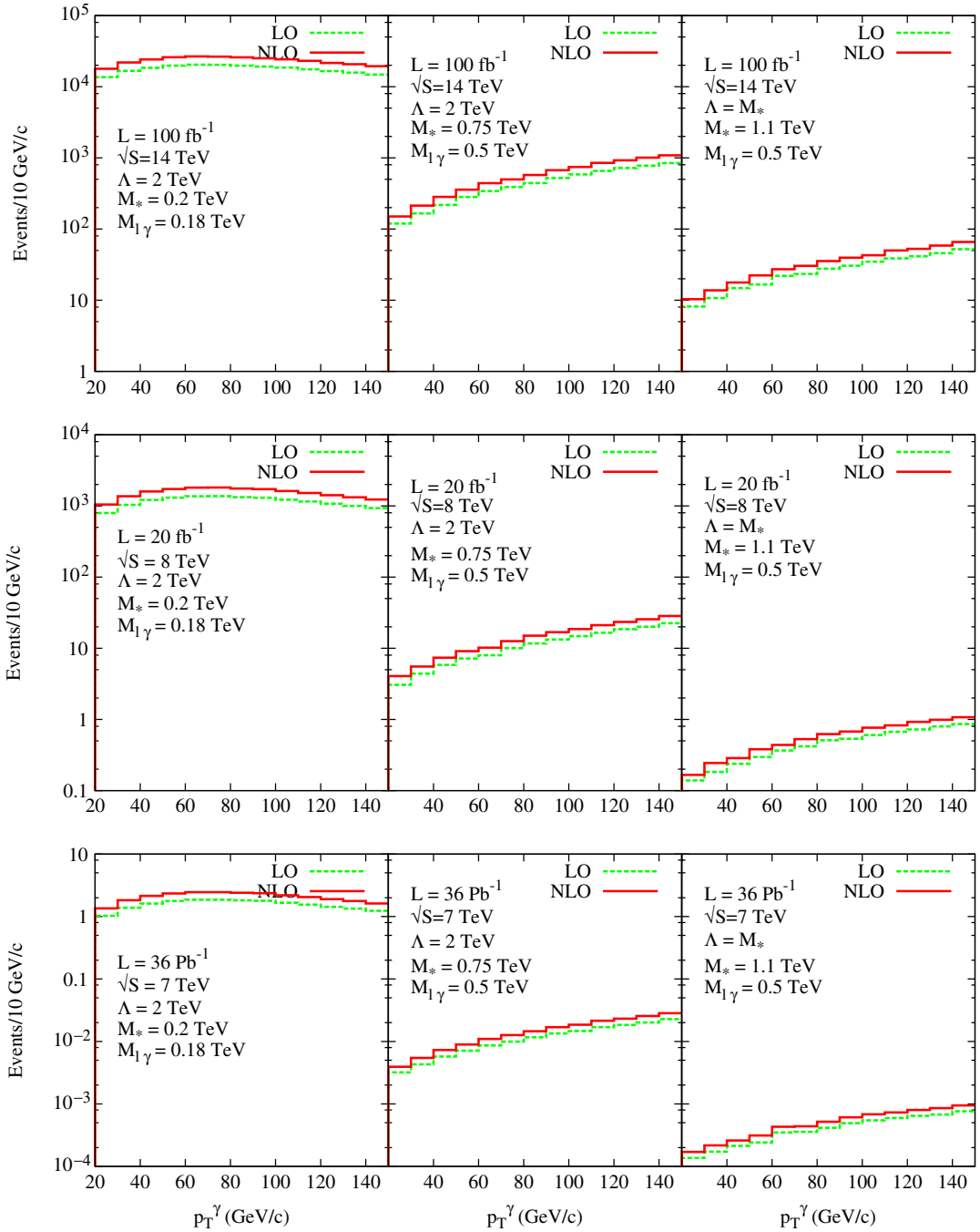

FIG. 7 (color online). Photon transverse momentum distribution at three different excited lepton masses and three different LHC energies for MSTW 2008 parton distribution functions.

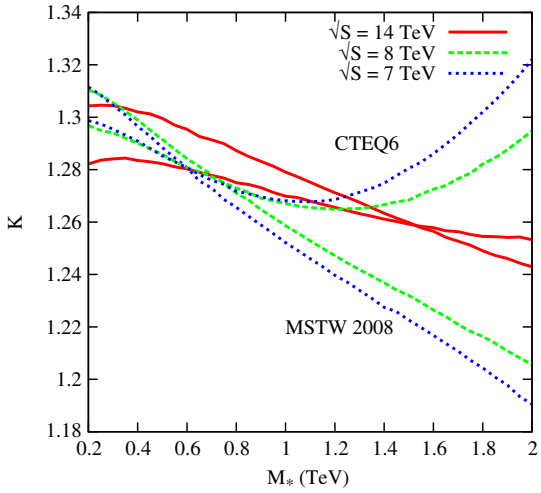

FIG. 8 (color online). K factor for $l\bar{l}\gamma$ production at three different LHC energies. The lower (upper) set is for MSTW 2008 (CTEQ6) parton distribution functions.

2008 [29] for two different values of the contact interaction scale ($\Lambda = 2$, 6 TeV). As before (and for identical reasons), the cross section decreases as the invariant mass M_* increases. From Fig. 5, we see that, as the contact interaction scale (Λ) increases, the cross section (both LO as well as NLO) decreases uniformly as Λ^{-4} as expected from Eq. (1). Therefore, one can obtain the cross section (for both LO as well as NLO) for arbitrary values of Λ by multiplying our results by an appropriate scale factor.

In Fig. 6, we plot a particular measurable, viz. the product of the cross section and the branching fraction, along with the 95% C.L. upper limit as obtained by the CMS Collaboration [13]. From this figure, it is clear that, on inclusion of NLO QCD corrections, the mass limit on the excited leptons is enhanced somewhat, which we quantify in Table II.

In Fig. 7, we display the photon transverse momentum distribution with the same lepton-photon invariant mass cut ($M_{l\gamma}^{\rm cut}$) as given in Ref. [13]. In this figure, we consider the projected luminosity 20(100) fb^{-1} at $\sqrt{S} = 8(14)$ TeV LHC energy. This figure demonstrates that the enhancement has a relatively small dependence on the photon p_T, and thus the language of the K factor is a useful one not only for effecting Monte Carlo studies of the process, but also for analyzing actual data.

We now turn to the dependence on the choice of the parton distributions. As Fig. 8 shows, the variation of K factor is about 20%–30% for both the PDFs, CTEQ6 and

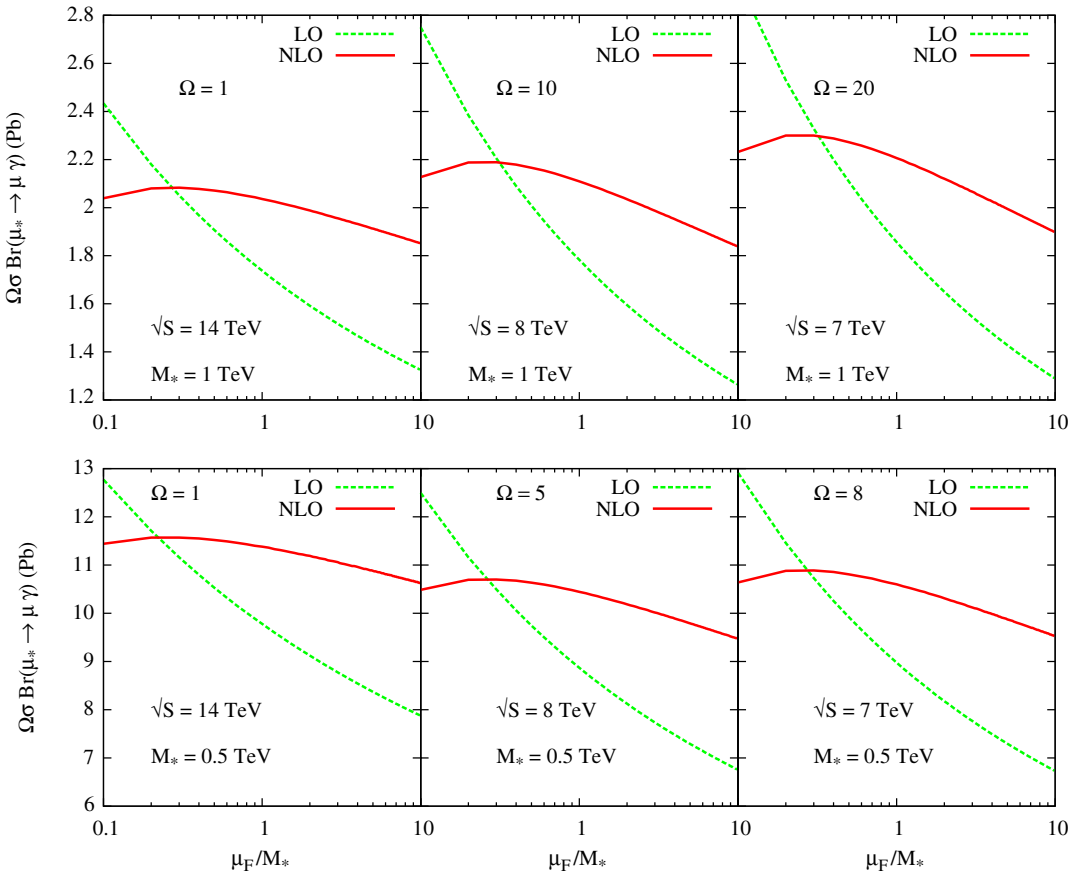

FIG. 9 (color online). Variation of the total cross section with respect to the factorization scale μ_F using CTEQ6 PDFs for $\Lambda = 2$ TeV. Here Ω is just a constant scale factor introduced to put all the graphs on the same frame of respective scale.

MSTW 2008. The major difference in K factor between the two PDFs (especially at low center of mass energy) is due to the different parametrization of their parton distribution function (owing to their use of different data sets to extract the PDFs). As can be expected, the difference is minor for low values of $M_*/\sqrt{S}$ (where experimental data abound and the understanding is better) and increases with the ratio. This difference is irreducible at present and can be reduced only on inclusion of either more data (and, hence, more refined PDFs) or the calculation of still higher-order effects.

In our above discussions, we have considered the simplest case $\mu_F^2 = \mu_R^2 = Q^2$ where the cross section depends only on physical scales like the c.o.m. energy ($\sqrt{S}$) and the masses of final state particles (M_*). Now we turn on another scale called the factorization scale μ_F^2 ($= \mu_R^2$ the renormalization scale), and we have shown the factorization scale dependence of our NLO result in Fig. 9. From this figure, it is clear that the scale dependence reduces greatly at the NLO cross section compare to the LO cross section. This signifies the necessity of NLO QCD corrections.

IV. CONCLUSIONS

In conclusion, we have systematically performed the next-to-leading-order QCD corrections for the $V \pm A$ type contact interactions as given in Eq. (1). As opposed to naive expectations, we have showed that the QCD corrections are meaningful and reliable even in such a nonrenormalizable theory.

We have analyzed the variation of the cross section with respect to the excited lepton mass (and, hence, the invariant mass of one SM lepton and a SM gauge boson) at the LHC. The enhancement of the NLO cross section over the LO cross section is found to be quite significant. To quantify the enhancement, we present the corresponding K factors in a form suitable for experimental analyses. A quick estimate shows that the inclusion of these corrections changes the mass exclusion limits by about 60 GeV.

As is well known, the cross section calculated at the leading order in perturbation theory suffers scale uncertainty on account of the arbitrariness in the choice of factorization and renormalization scales. These uncertainties are due to the absence of higher-order contributions in the calculations. On inclusion of each higher order, these scale uncertainties reduce gradually, and the predictions are expected to become more reliable. This is explicitly borne out by our calculations, which demonstrate that the scale dependence of the NLO result is greatly reduced in comparison to that for the LO case.

ACKNOWLEDGMENTS

The author thanks Debajyoti Choudhury for useful discussions and comments. The author also acknowledges Satyaki Bhattacharya for useful discussions. This work was supported by the CSIR Pool Scheme (Pool No. 8545-A), India.

[1] H. P. Nilles, Phys. Rep. **110**, 1 (1984); H. E. Haber and G. L. Kane, Phys. Rep. **117**, 75 (1985); in *Perspectives in Supersymmetry*, edited by G. L. Kane (World Scientific, Singapore, 1998); M. Drees, R. M. Godbole, and P. Roy, *Theory and Phenomenology of Sparticles* (World Scientific, Singapore, 2005).

[2] J. C. Pati and A. Salam, Phys. Rev. D **10**, 275 (1974).

[3] H. Georgi and S. L. Glashow, Phys. Rev. Lett. **32**, 438 (1974); P. Langacker, Phys. Rep. **72**, 185 (1981).

[4] E. Eichten, K. D. Lane, and M. E. Peskin, Phys. Rev. Lett. **50**, 811 (1983); E. Eichten, I. Hinchliffe, K. D. Lane, and C. Quigg, Rev. Mod. Phys. **56**, 579 (1984).

[5] J. C. Pati, A. Salam, and J. A. Strathdee, Phys. Lett. **59B**, 265 (1975); H. Fritzsch and G. Mandelbaum, Phys. Lett. **102B**, 319 (1981); W. Buchmuller, R. D. Peccei, and T. Yanagida, Phys. Lett. **124B**, 67 (1983); Nucl. Phys. **B227**, 503 (1983); **B231**, 53 (1984); U. Baur and H. Fritzsch, Phys. Lett. **134B**, 105 (1984); X. Li and R. E. Marshak, Nucl. Phys. **B268**, 383 (1986); I. Bars, J. F. Gunion, and M. Kwan, Nucl. Phys. **B269**, 421 (1986); G. Domokos and S. Kovesi-Domokos, Phys. Lett. B **266**, 87 (1991); J. L. Rosner and D. E. Soper, Phys. Rev. D **45**, 3206 (1992); M. A. Luty and R. N. Mohapatra, Phys. Lett. B **396**, 161 (1997); K. Hagiwara, K. Hikasa, and M. Tanabashi, Phys. Rev. D **66**, 010001 (2002); Phys. Lett. B **592**, 1 (2004).

[6] For a review and additional references, see R. R. Volkas and G. C. Joshi, Phys. Rep. **159**, 303 (1988).

[7] H. Harari and N. Seiberg, Phys. Lett. **98B**, 269 (1981); M. E. Peskin, in *Proceedings of the 1981 International Symposium on Lepton and Photon Interaction at High Energy*, edited by W. Pfeil (1981), p. 880; L. Lyons, Oxford University Publication 52/82, 1982; G. 't Hooft, in *Recent Developments in Gauge Theories* (Plenum, New York, 1980).

[8] U. Baur, M. Spira, and P. Zerwas, Phys. Rev. D **42**, 815 (1990); J. Kuhn and P. Zerwas, Phys. Lett. **147B**, 189 (1984).

[9] F. Boudjema, A. Djouadi, and J. Kneur, Z. Phys. C **57**, 425 (1993); K. Hagiwara, D. Zeppenfeld, and S. Komamiya, Z. Phys. C **29**, 115 (1985); N. Cabibbo, L. Maiani, and Y. Srivastava, Phys. Lett. **139B**, 459 (1984).

[10] ALEPH Collaboration, Phys. Lett. B **385**, 445 (1996); OPAL Collaboration, Eur. Phys. J. C **14**, 73 (2000); L3 Collaboration, Phys. Lett. B **568**, 23 (2003); DELPHI Collaboration, Eur. Phys. J. C **8**, 41 (1999); DELPHI Collaboration, Eur. Phys. J. C **46**, 277 (2006).

[11] H1 Collaboration, Phys. Lett. B **678**, 335 (2009); H1 Collaboration, Phys. Lett. B **666**, 131 (2008); C. Adloff *et al.*, Eur. Phys. J. C **17**, 567 (2000); S. Chekanov *et al.* (ZEUS Collaboration), Phys. Lett. B **549**, 32 (2002).
[12] CDF Collaboration, Phys. Rev. Lett. **94**, 101802 (2005); CDF Collaboration, Phys. Rev. Lett. **97**, 191802 (2006); D0 Collaboration, Phys. Rev. D **73**, 111102 (2006); D0 Collaboration, Phys. Rev. D **77**, 091102 (2008).
[13] CMS Collaboration, Phys. Lett. B **704**, 143 (2011).
[14] ATLAS Collaboration, Phys. Rev. D **85**, 072003 (2012).
[15] J. L. Diaz and O. A. Sampayo, Phys. Rev. D **49**, R2149 (1994).
[16] J. I. Aranda, R. Martinez, and O. A. Sampayo, Phys. Rev. D **62**, 013010 (2000).
[17] wS. D. Drell and T.-M. Yan, Phys. Rev. Lett. **25**, 316 (1970); J. H. Christenson, G. S. Hicks, L. M. Lederman, P. J. Limon, and B. G. Pope, *ibid.* **25**, 1523 (1970); L. M. Lederman and B. G. Pope, *ibid.* **27**, 765 (1971).
[18] R. Hamberg, W. L. van Neerven, and T. Matsuura, Nucl. Phys. **B359**, 343 (1991).
[19] P. J. Sutton, A. D. Martin, R. G. Roberts, and W. J. Stirling, Phys. Rev. D **45**, 2349 (1992); A. D. Martin, W. J. Stirling, and R. G. Roberts, Phys. Lett. B **354**, 155 (1995).
[20] W. T. Giele, E. W. N. Glover, and D. A. Kosower, Nucl. Phys. **B403**, 633 (1993).
[21] G. Corcella, I. G. Knowles, G. Marchesini, S. Moretti, K. Odagiri, P. Richardson, M. H. Seymour, and B. R. Webber, J. High Energy Phys. 01 (2001) 010.
[22] D. Choudhury, S. Majhi, and V. Ravindran, J. High Energy Phys. 01 (2006) 027.
[23] P. Mathews, V. Ravindran, K. Sridhar, and W. L. van Neerven, Nucl. Phys. **B713**, 333 (2005).
[24] S. Majhi *et al.* (unpublished).
[25] G. Altarelli, R. K. Ellis, and G. Martinelli, Nucl. Phys. **B157**, 461 (1979); B. Humpert and W. L. van Neerven, Phys. Lett. **84B**, 327 (1979); **85B**, 293 (1979); **89B**, 69 (1979); Nucl. Phys. **B184**, 225 (1981); J. Kubar, M. le Bellac, J. L. Meunier, and G. Plaut, Nucl. Phys. **B175**, 251 (1980); P. Aurenche and P. Chiapetta, Z. Phys. C **34**, 201 (1987); P. J. Sutton, A. D. Martin, R. G. Roberts, and W. J. Stirling, Phys. Rev. D **45**, 2349 (1992); P. J. Rijken and W. L. van Neerven, Phys. Rev. D **51**, 44 (1995).
[26] J. Pumplin, D. R. Stump, J. Huston, H. L. Lai, P. M. Nadolsky, and W. K. Tung, J. High Energy Phys. 07 (2002) 012.
[27] O. J. P. Eboli, S. M. Lietti, and P. Mathews, Phys. Rev. D **65**, 075003 (2002).
[28] S. C. Inan, Phys. Rev. D **81**, 115002 (2010).
[29] A. D. Martin, W. J. Stirling, R. S. Thorne, and G. Watt, Eur. Phys. J. C **63**, 189 (2009).